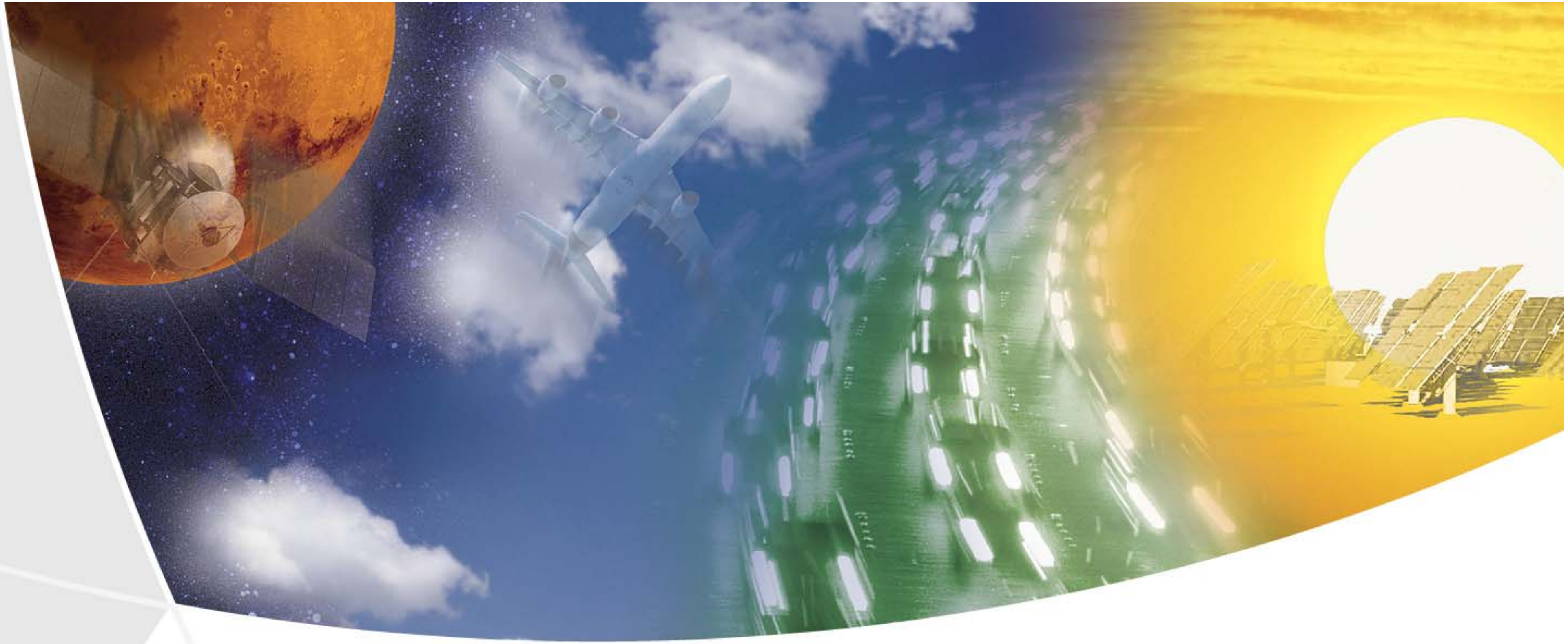

Development of Nano-Structured Solid Oxide Fuel Cell Electrodes

G. Schiller, S.A. Ansar, M. Müller

German Aerospace Center (DLR), Institute of Technical Thermodynamics,
Pfaffenwaldring 38-48, D-70569 Stuttgart, Germany

17th Annual International Conference on Composites/Nano Engineering (ICCE-17),
Honolulu, July 26-31, 2009

Deutsches Zentrum
DLR für Luft- und Raumfahrt e.V.
in der Helmholtz-Gemeinschaft

Outline

- **Introduction**
  - Principle of planar SOFC
  - DLR spray concept for SOFC
- **Nanostructured Cathode by using RF Plasma Technology (TPCVD)**
  - Deposition from liquid precursors
  - Phase purity
  - Structure
- **Nanostructured Anode by using DC Plasma Technology**
  - Agglomerated nanoparticles
  - Suspension plasma spraying (SPS)
  - Solution precursor plasma spraying (SPPS)
- **Conclusion**

Design and Principle of a Planar SOFC

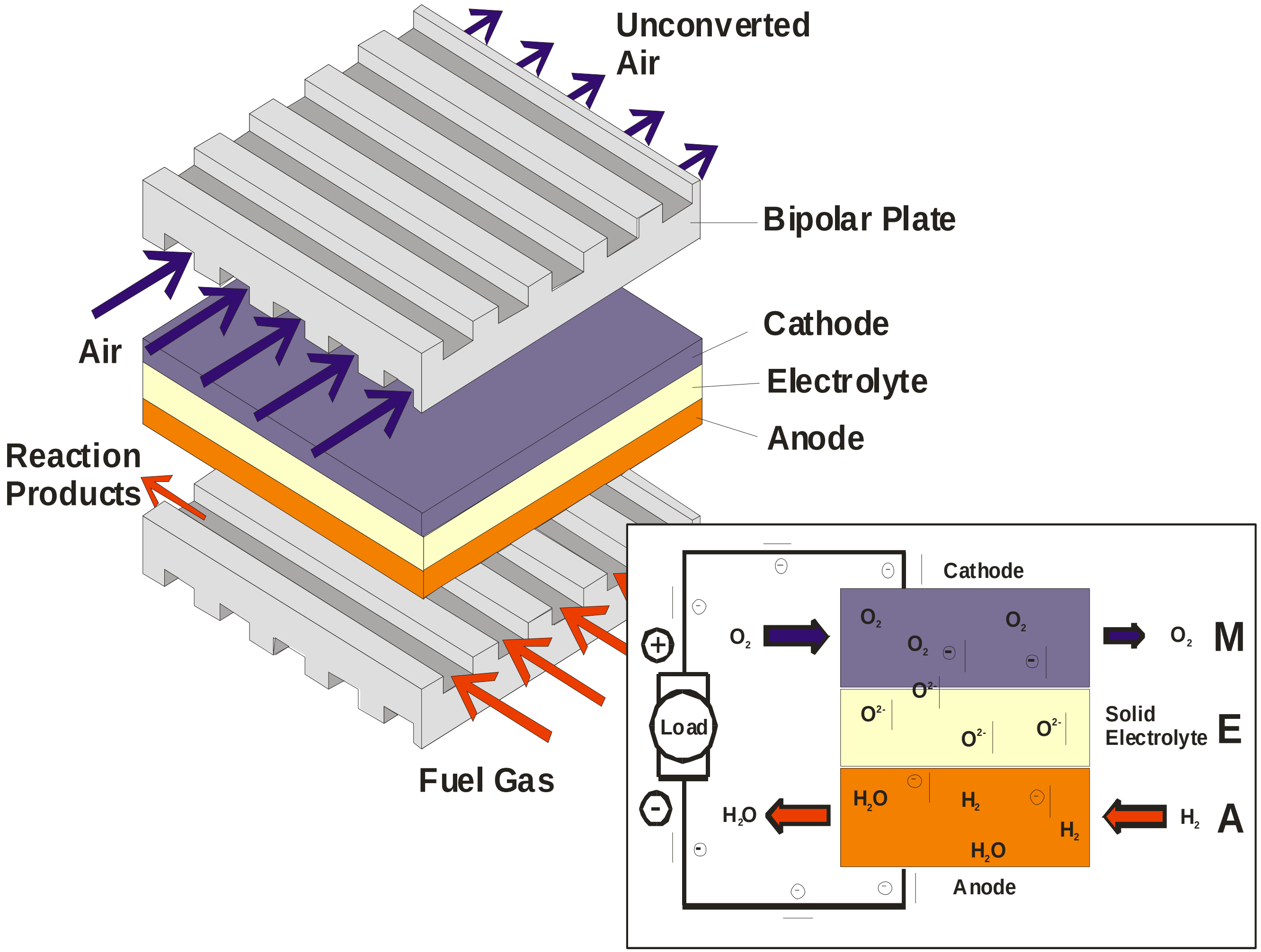

SOFC Metal-Supported Cell

Plasma Deposition Technology

Thin-Film Cells

Ferritic Substrates and Interconnects

Compact Design with Thin Metal Sheet Substrates

Brazing, Welding and Glass Seal as Joining and Sealing Technology

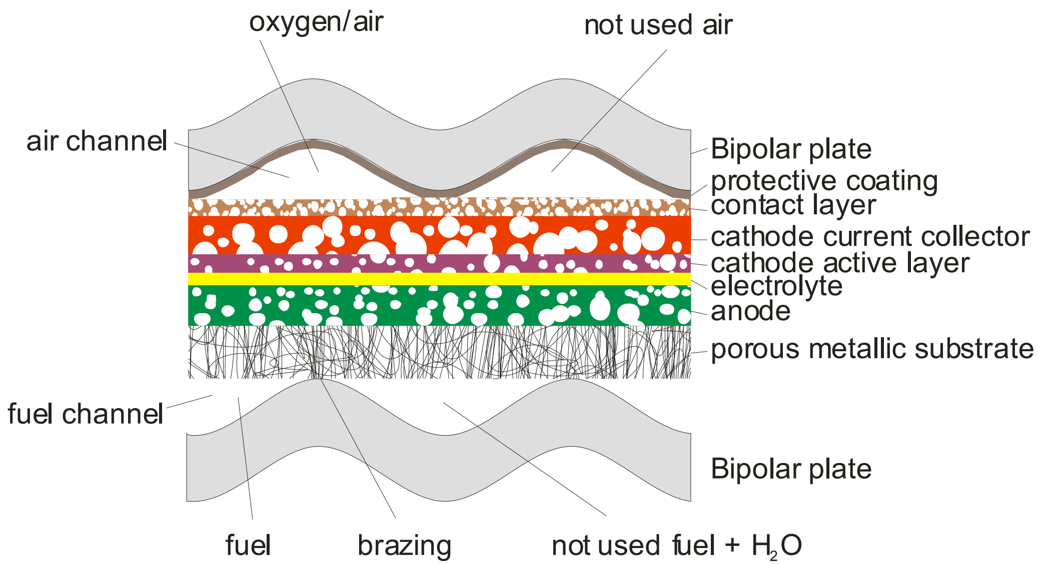

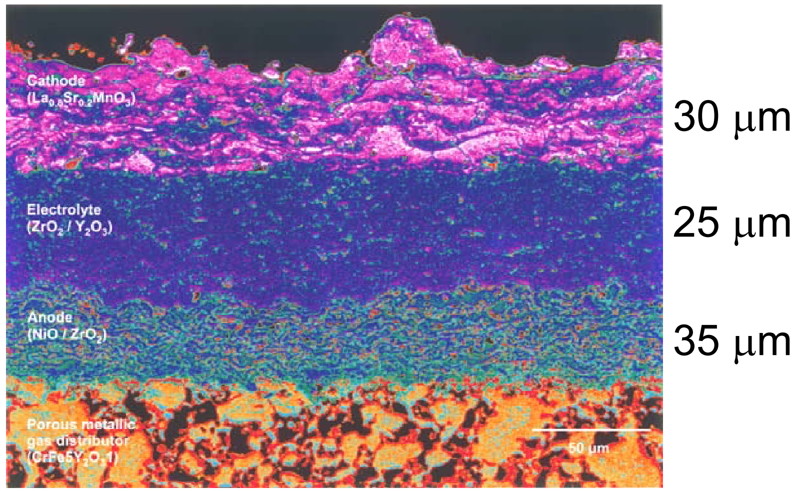

(not in scale)

Plasma Spray Laboratory at DLR Stuttgart

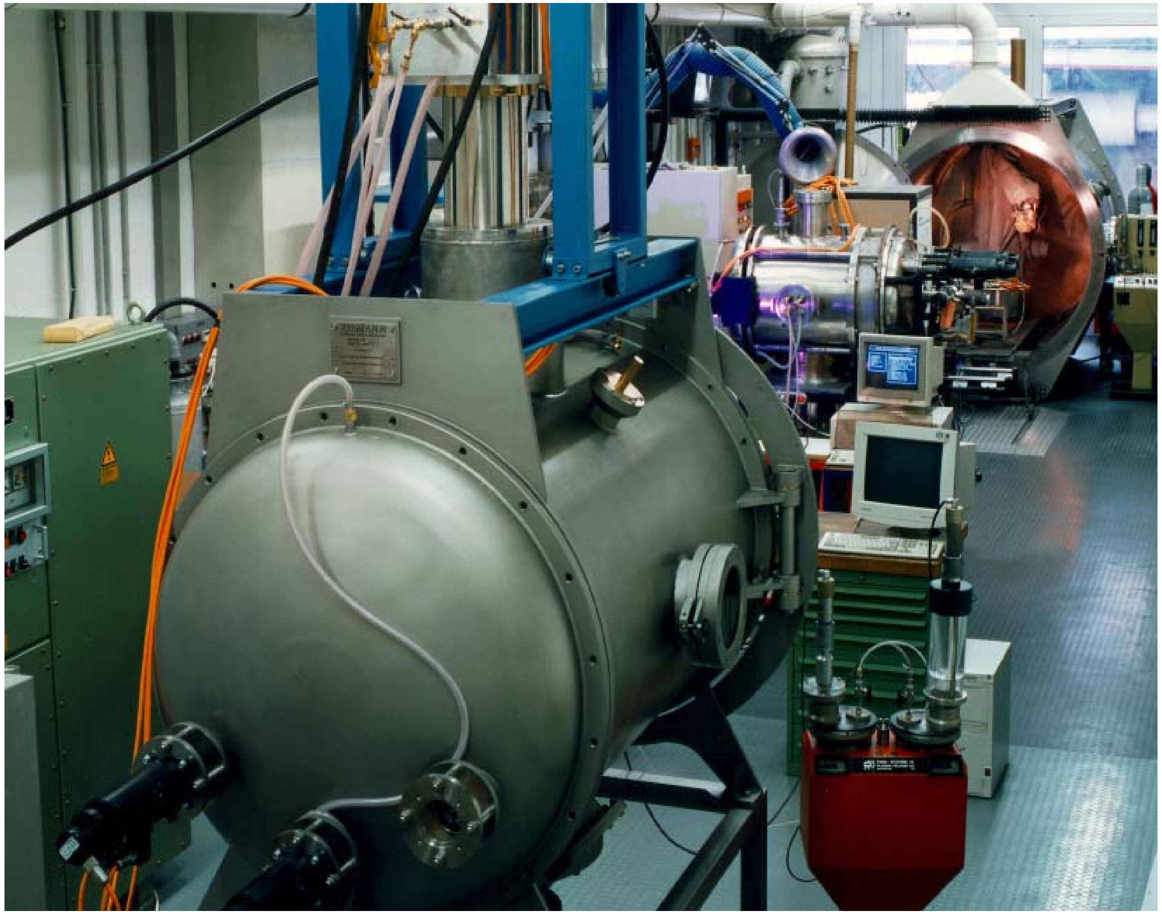

Experimental Setup

Atomization

Tasks:

spray angle 10-20°
homogeneous spray
(narrow droplet size distribution)

Problems:

small dimensions
extremely high temperature

Present solution:

“air assist atomizer”:
disintegration of liquid
stream in gas jet

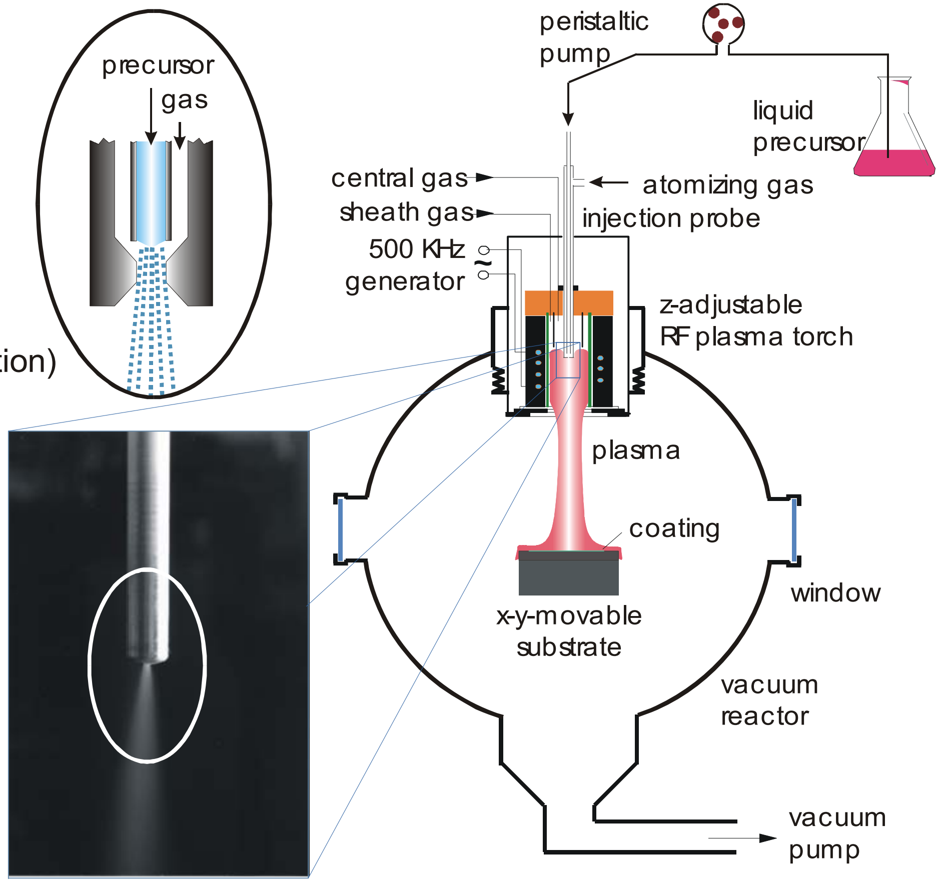

Applied Precursor Solutions and Desired Synthesis Products

	Synthesis product	Precursor	Concentration
A	$La_{0.9}Sr_{0.1}MnO_3$ (LSM)	$La(NO_3)_3 \cdot 6\,H_2O$ $Sr(NO_3)_2$ $Mn(NO_3)_2 \cdot 4\,H_2O$	0,9 M 0,1 M 1,0 M
B	$La_{0.5}Sr_{0.5}MnO_3$ (LSM)	$La(NO_3)_3 \cdot 6\,H_2O$ $Sr(NO_3)_2$ $Mn(NO_3)_2 \cdot 4\,H_2O$	0,5 M 0,5 M 1,0 M
C	$La_{0.65}Sr_{0.3}MnO_3$ (ULSM)	$La(NO_3)_3 \cdot 6\,H_2O$ $Sr(NO_3)_2$ $Mn(NO_3)_2 \cdot 4\,H_2O$	0,65 M 0,3 M 1,0 M
D	$Pr_{0.65}Sr_{0.3}MnO_3$ (UPSM)	$Pr(NO_3)_3 \cdot 5\,H_2O$ $Sr(NO_3)_2$ $Mn(NO_3)_2 \cdot 4\,H_2O$	0,65 M 0,3 M 1,0 M
E	$La_{0.8}Sr_{0.2}FeO_3$ (LSF)	$La(NO_3)_3 \cdot 6\,H_2O$ $Sr(NO_3)_2$ $Fe(NO_3)_3 \cdot 9\,H_2O$	0,8 M 0,2 M 1,0 M
F	$La_{0.8}Sr_{0.2}(Co,Fe)O_3$ (LSCF)	$La(NO_3)_3 \cdot 6\,H_2O$ $Sr(NO_3)_2$ $Co(NO_3)_2 \cdot 6\,H_2O$ $Fe(NO_3)_3 \cdot 9\,H_2O$	0,8 M 0,2 M 0,5 M 0,5 M
G	$La_{0.58}Sr_{0.4}Fe_{0.8}Co_{0.2}O_3$ (LSFC)	$La(NO_3)_3 \cdot 6\,H_2O$ $Sr(NO_3)_2$ $Fe(NO_3)_3 \cdot 9\,H_2O$ $Co(NO_3)_2 \cdot 6\,H_2O$	0,58 M 0,4 M 0,8 M 0,2 M
H	$Pr_{0.58}Sr_{0.4}Fe_{0.8}Co_{0.2}O_3$ (PSFC)	$Pr(NO_3)_3 \cdot 5\,H_2O$ $Sr(NO_3)_2$ $Fe(NO_3)_3 \cdot 9\,H_2O$ $Co(NO_3)_2 \cdot 6\,H_2O$	0,58 M 0,4 M 0,8 M 0,2 M

X-Ray Diffraction Patterns of $La_{0.9}Sr_{0.1}MnO_3$

LaMn perovskite

Key parameter:

Mn loss depends on radial distance from plasma jet axis

Top:
TPCVD coating from central part of plasma jet

Bottom:
TPCVD coating from cooler margin

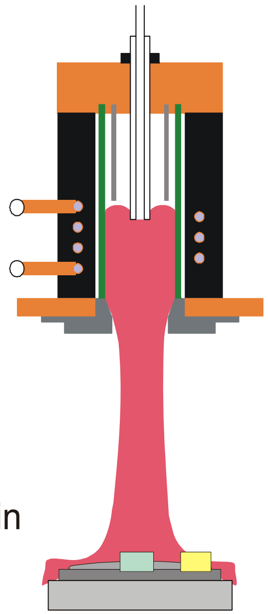

stationary substrate

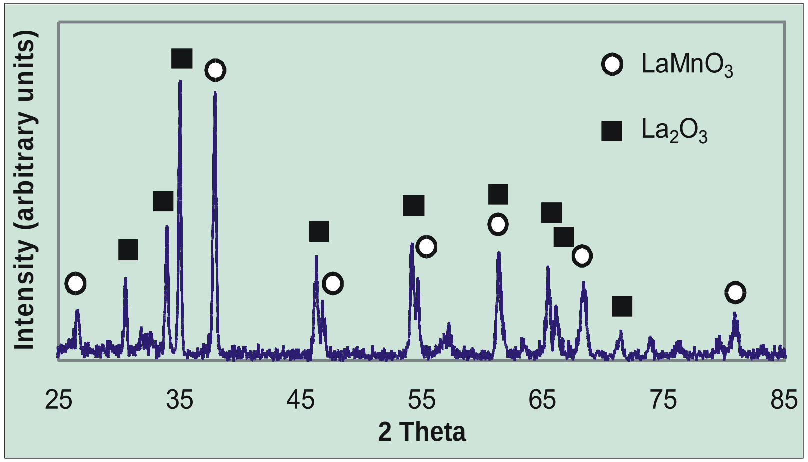

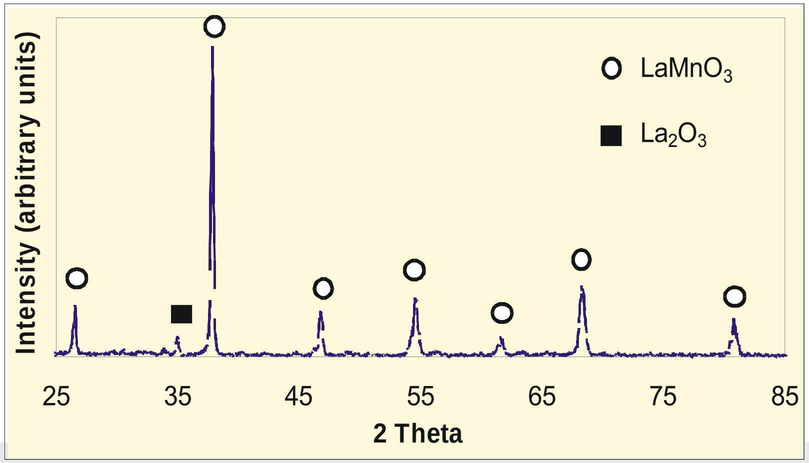

X-Ray Diffraction Patterns of $Pr_{0.58}Sr_{0.4}Fe_{0.8}Co_{0.2}O_3$

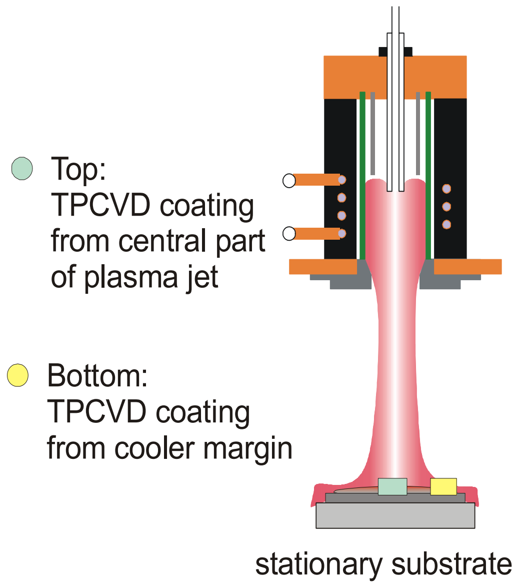

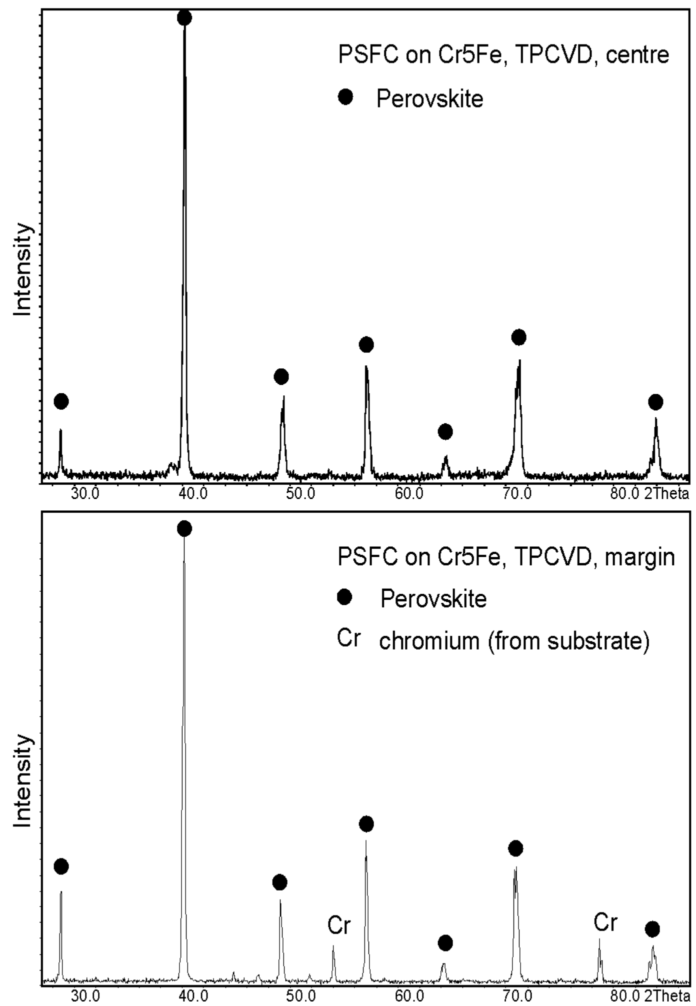

Microstructure of TPCVD Perovskite Coatings

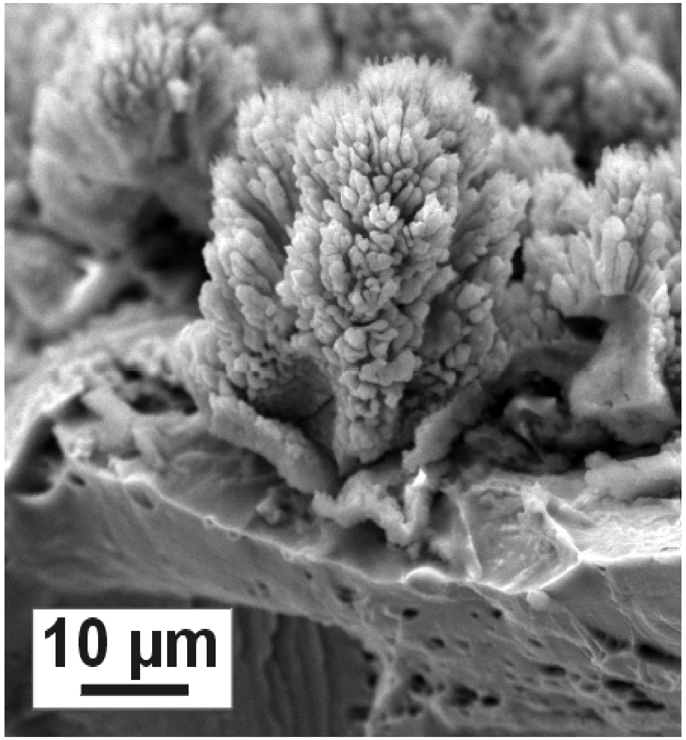

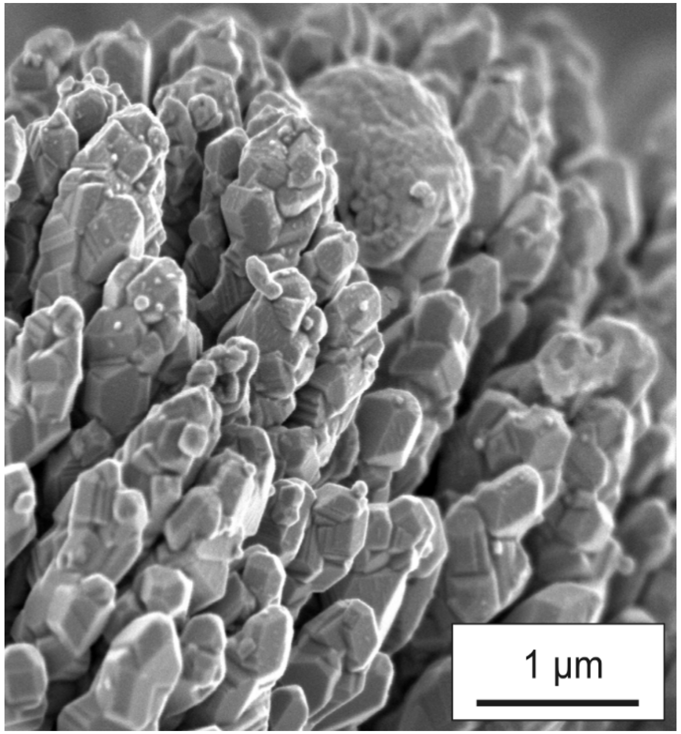

Functional Principle of DC Plasma

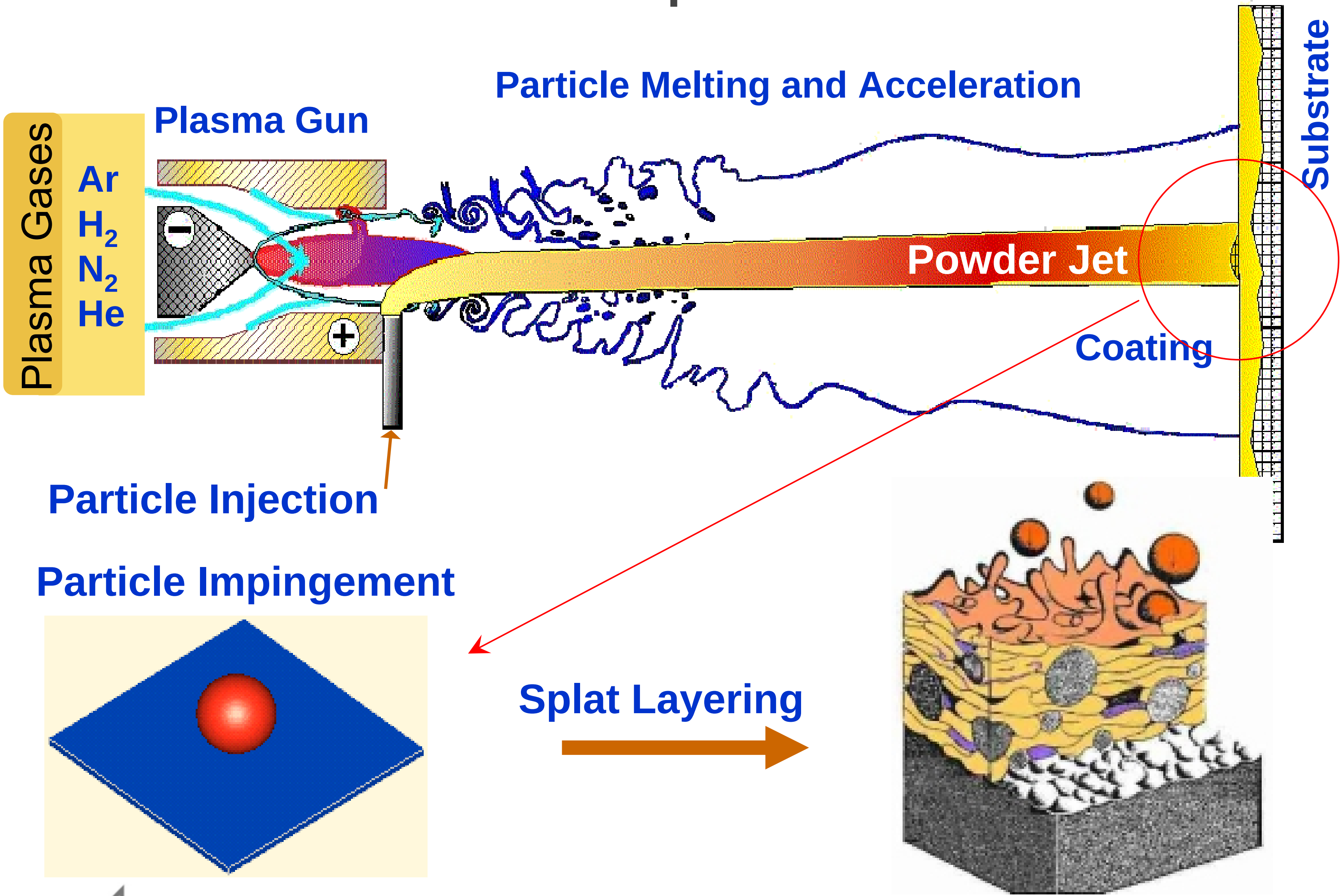

Vacuum Plasma Spraying of SOFC Cells

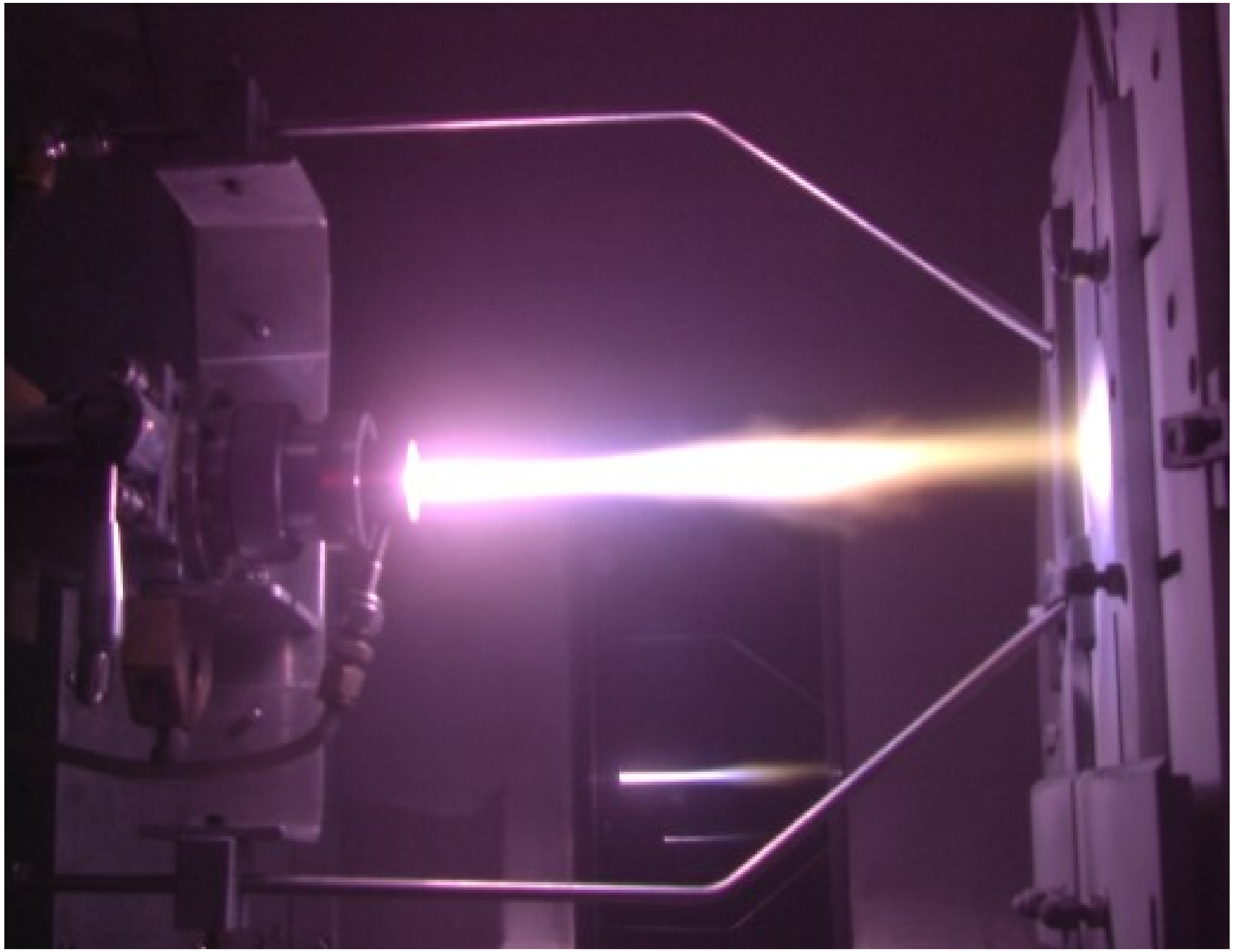

Feedstock Powder for DC Plasma Spraying

NiO+YSZ Powder

Co-precipitation and Spray-Drying

22 vol%NiO + YSZ

Agglomerated

Agglomerate size: -50+10 µm

Primary particle size: 20-80 nm

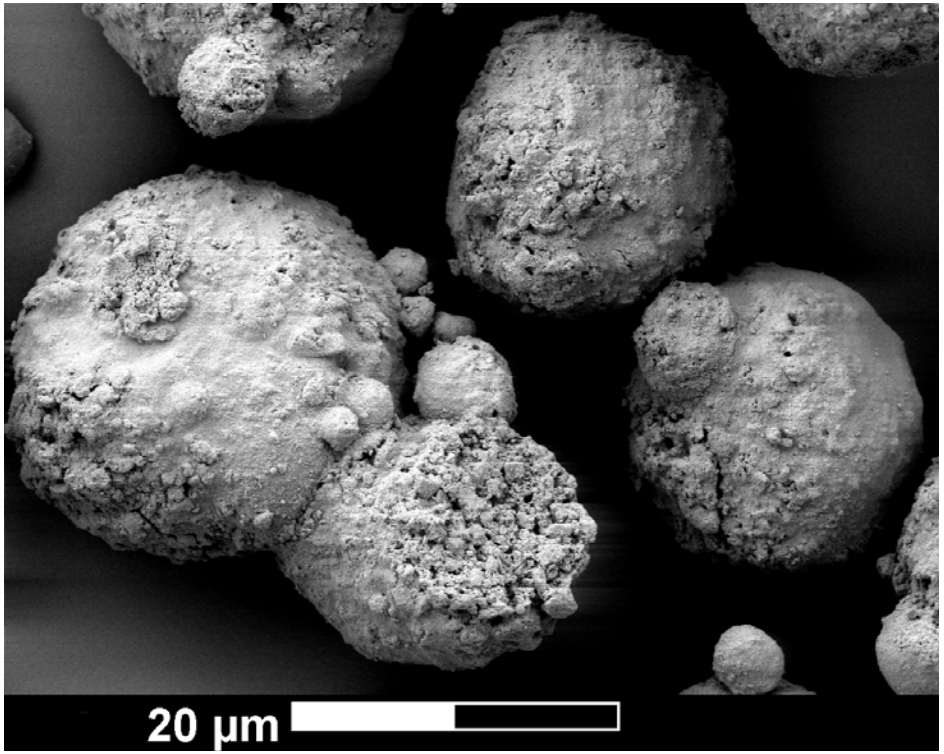

As-Sprayed Anode Structure and XRD

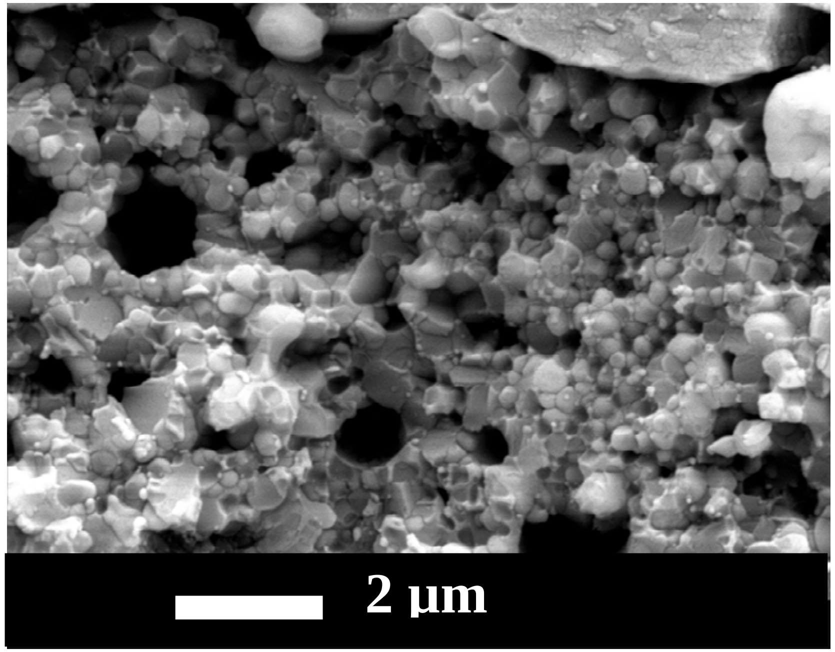

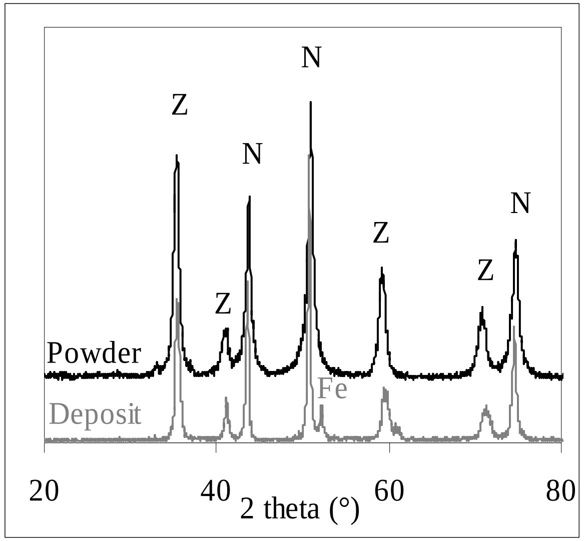

N= Ni(II)O

Z= Cubic-zirconia

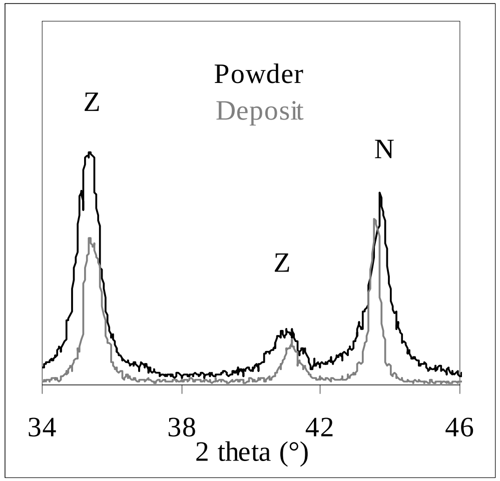

NiO+YSZ Plasma Sprayed Deposit

Particle size in deposit was 60-220 nm compared to 20-80 nm for the feedstock powder

Ni(II)O and cubic-YSZ were the phases detected by XRD

Permeability of Anode

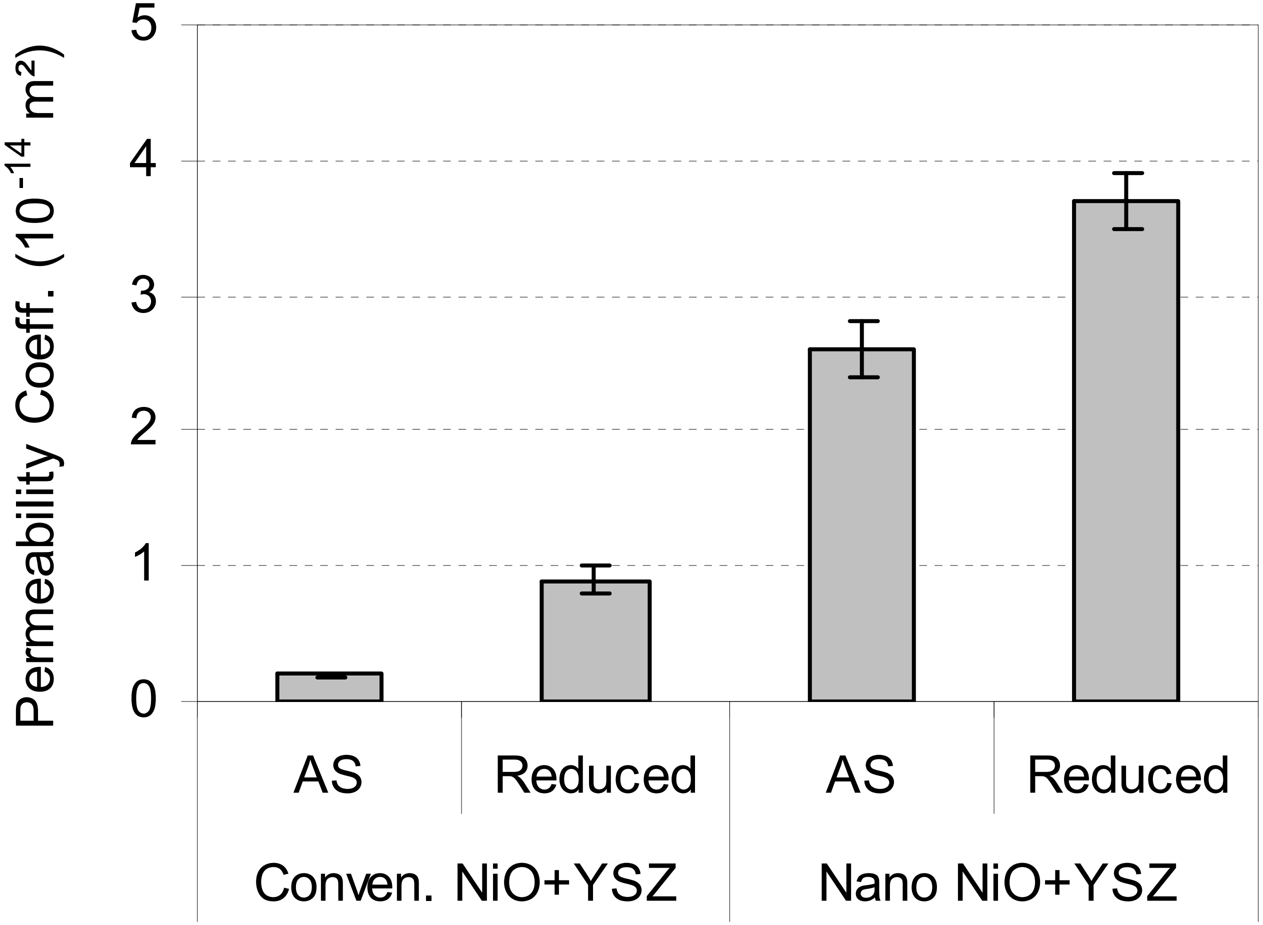

Conductivity of Nano-Anode

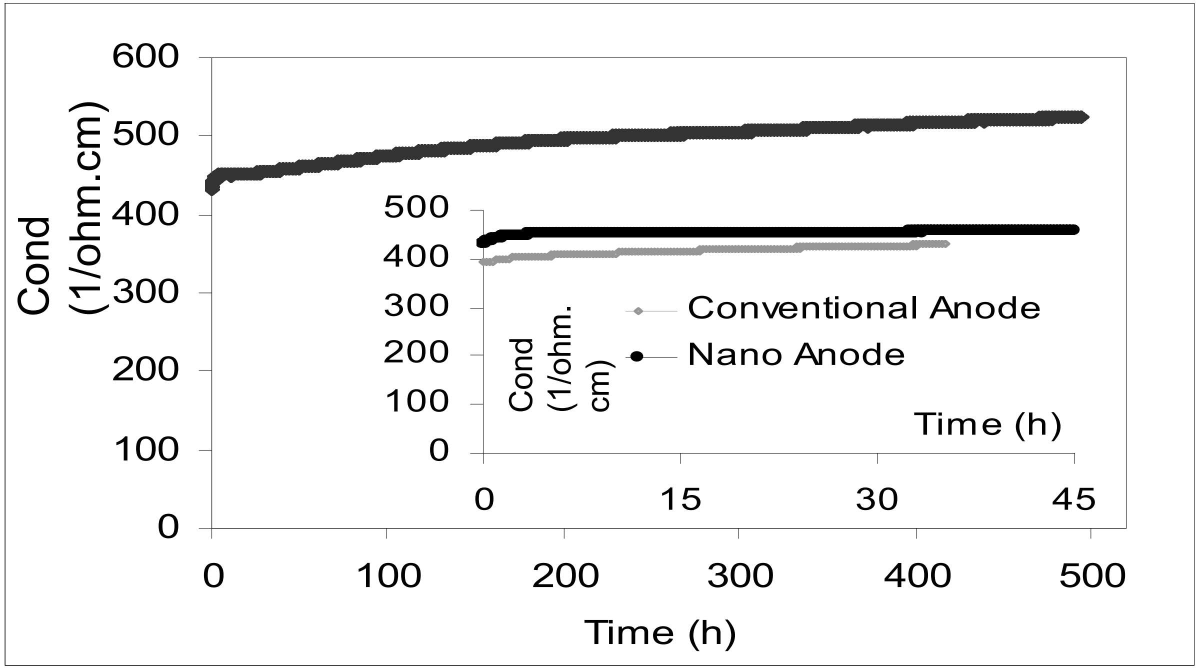

Test Atmosphere

2 slm Ar+5 vol% H_2

Conductivity of nano and conventional anode were comparable for first 30 to 40 hrs

Conductivity of nano anode increased for extended period of test time
- possible cause could be Ni particles phase I sintering

Electrochemical Testing

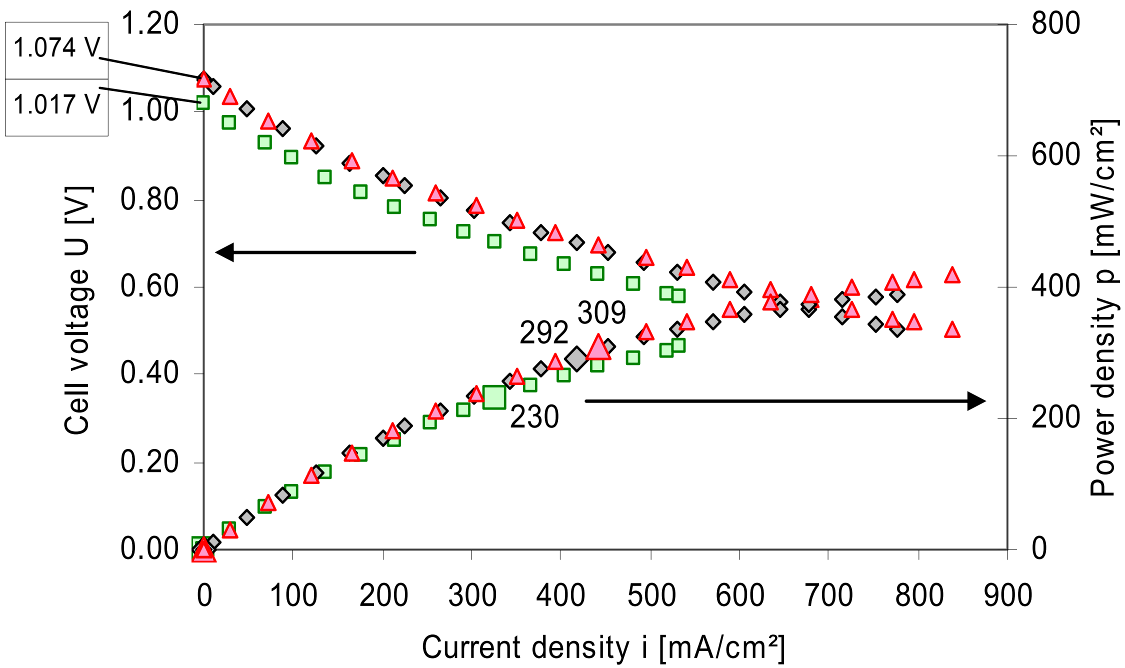

Reference cell with conventional anode (□); Cell with nanostructured anode after 100 h (Δ) and after 1500 h (◊) of operation
800°C - Cell area 12.6 cm² - Gases: 0.5 slm H_2+0.5 slm N_2/2.0 slm air).

- Cells containing a nano anode show 34% higher power density
- Anodic polarization at OCV of nano anode was 0.42 Ωcm² instead of 0.72 Ωcm² for conventional anode
- 3.33%/kh degradation rate for cells with nano anode is comparable to cells having conventional anodes – No evidence of additional degradation due to nanomaterials

Nano Anode Structure after SOFC Operation

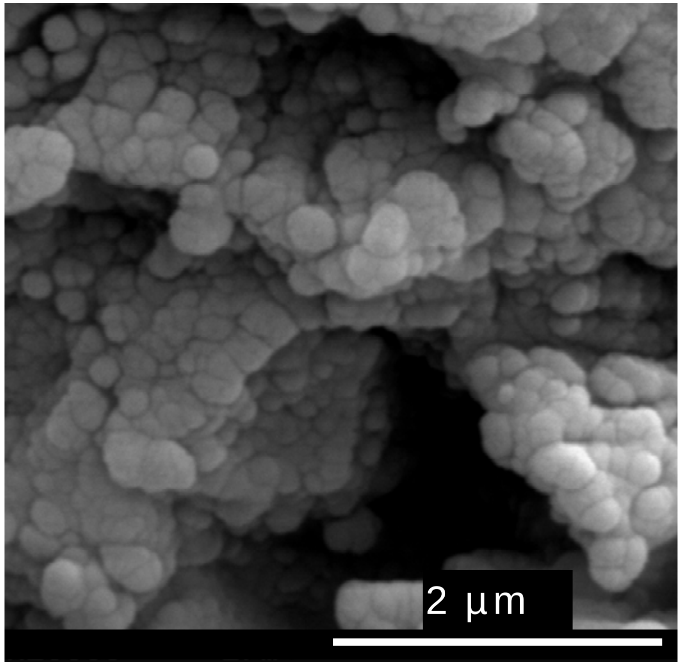

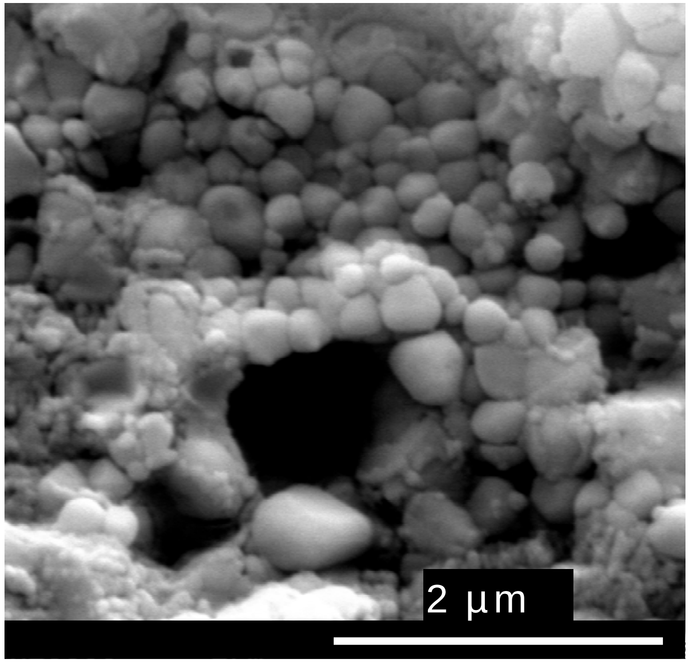

After 100 h of operation

After 1500 h of operation

Limited grain growth and sintering
Particle size: 60 to 220 nm after 100 h and 95 to 390 nm after 1500 h
Expected mechanisms are phase I or gas-phase sintering

Suspension and Solution Precursor Plasma Spraying

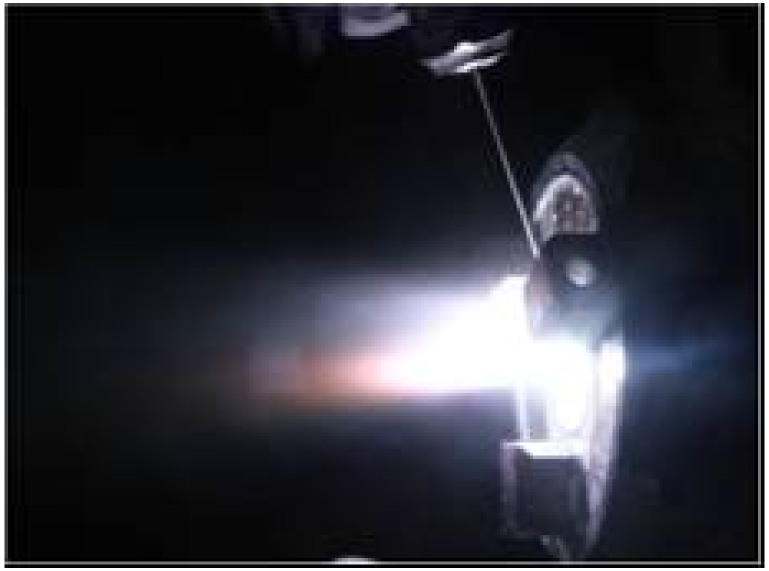

Suspension Plasma Spraying
Injection of nano-particles in plasma by suspending them in a liquid.

Solution Precursor Plasma Spraying
In-flight nano-particles synthesis by chemical reaction of metal salt precursors in plasma.

Suspension Plasma Spraying

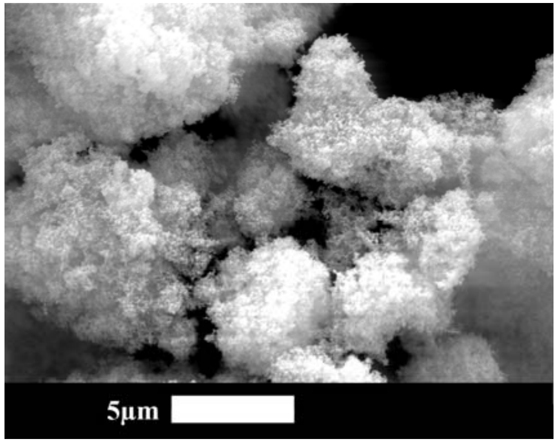

YSZ 40 nm particles and development of stable suspension using Zeta potential

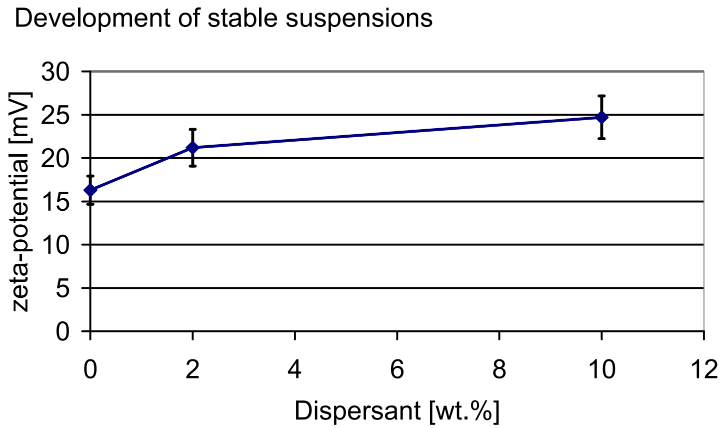

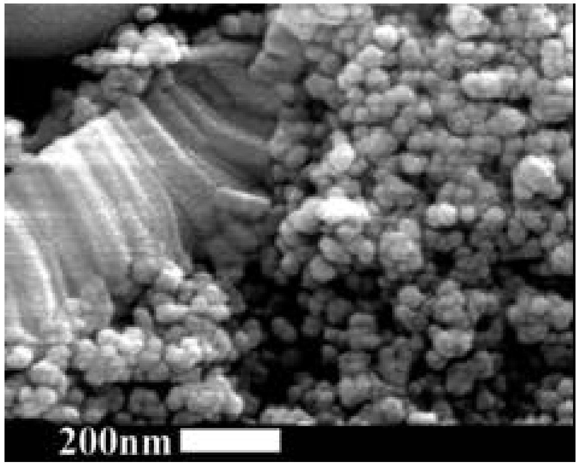

Nanostructured porous YSZ deposit
Porosity 35%

Outlook:
Additon of NiO for anode and LSM for cathode

Conclusion

- Nanostructured cathodes and anodes for SOFC were prepared by applying plasma deposition processes (RF and DC plasma)
- Two approaches were applied:
  - Introduction of pre-synthesized nanoparticles as agglomerates or suspensions into the plasma
  - In-situ synthesis of nanomaterials and deposits from solutions of metal salts
- TPCVD cathodes initially exhibited undesired secondary phases which was overcome by adjusting the chemical composition of the precursor material. The microstructure was columnar type with very high open porosity
- For 1500 hours of operation only limited growth of nanosized particles was observed in SOFC anodes
- Further improvement of the microstructure of anodes is in progress using DC plasma suspension and solution precursor plasma spraying

Synthesis from Liquid Precursors in an RF Plasma

Why r.f. plasma?

large volume, low jet velocity,
i.e. more complete synthesis

axial material injection

electrodeless, i.e. oxidizing
conditions possible

Why liquid precursors?

cost reduction

continuous feeding of material

homogeneous distribution in the plasma

synthesis of thermally instable materials

simple adjustment of stoichiometry

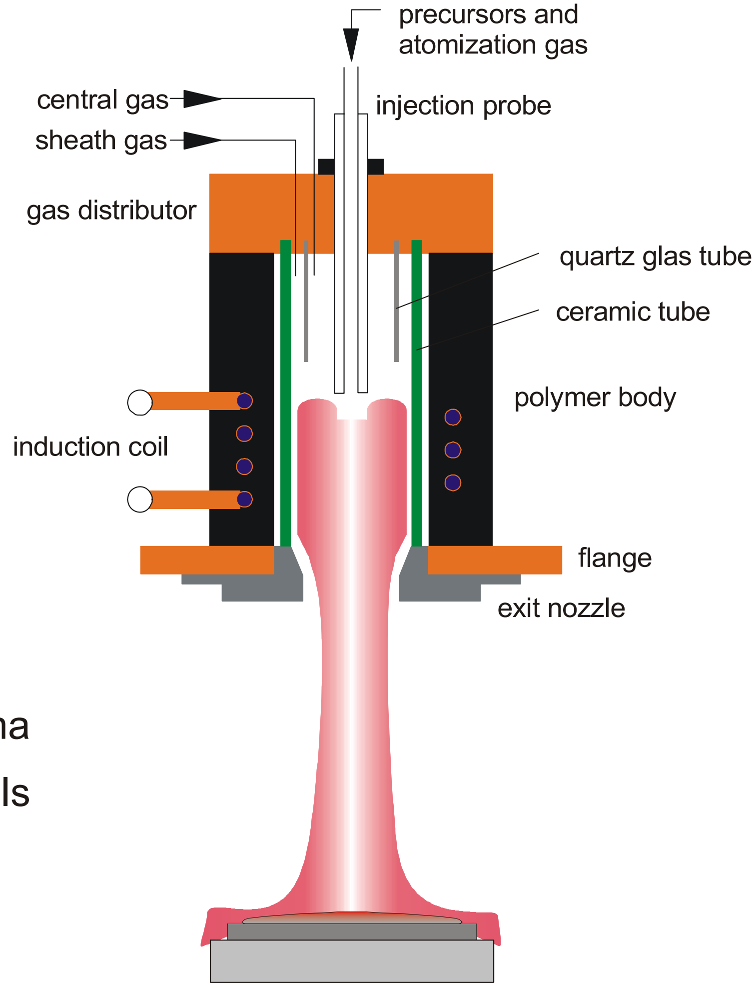

X-Ray Diffraction Patterns of $La_{0.58}Sr_{0.4}Fe_{0.8}Co_{0.2}O_3$

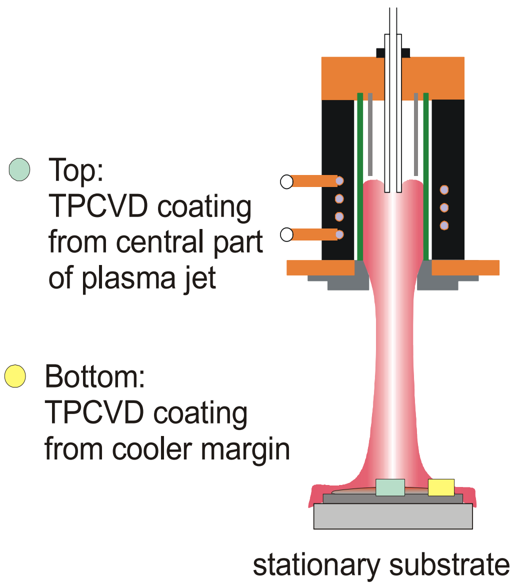

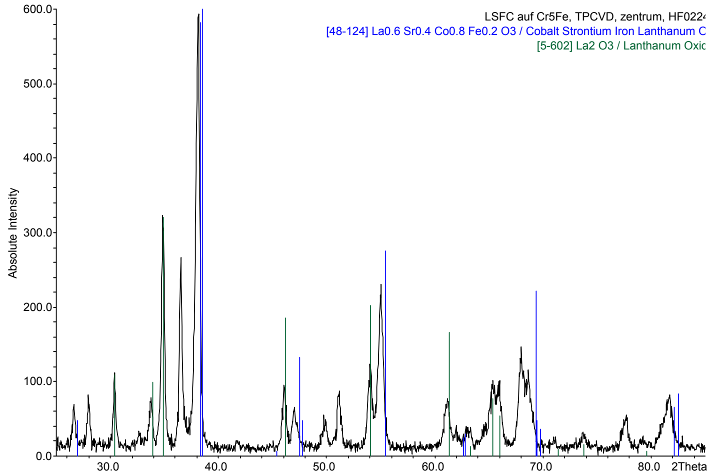

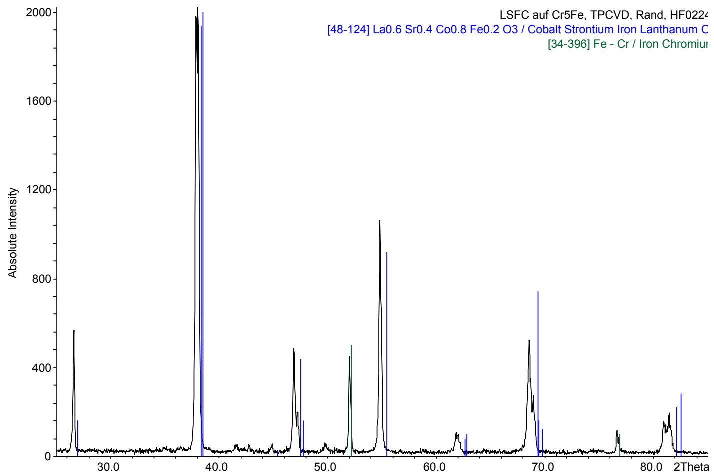

Electrical Conductivity Measurement

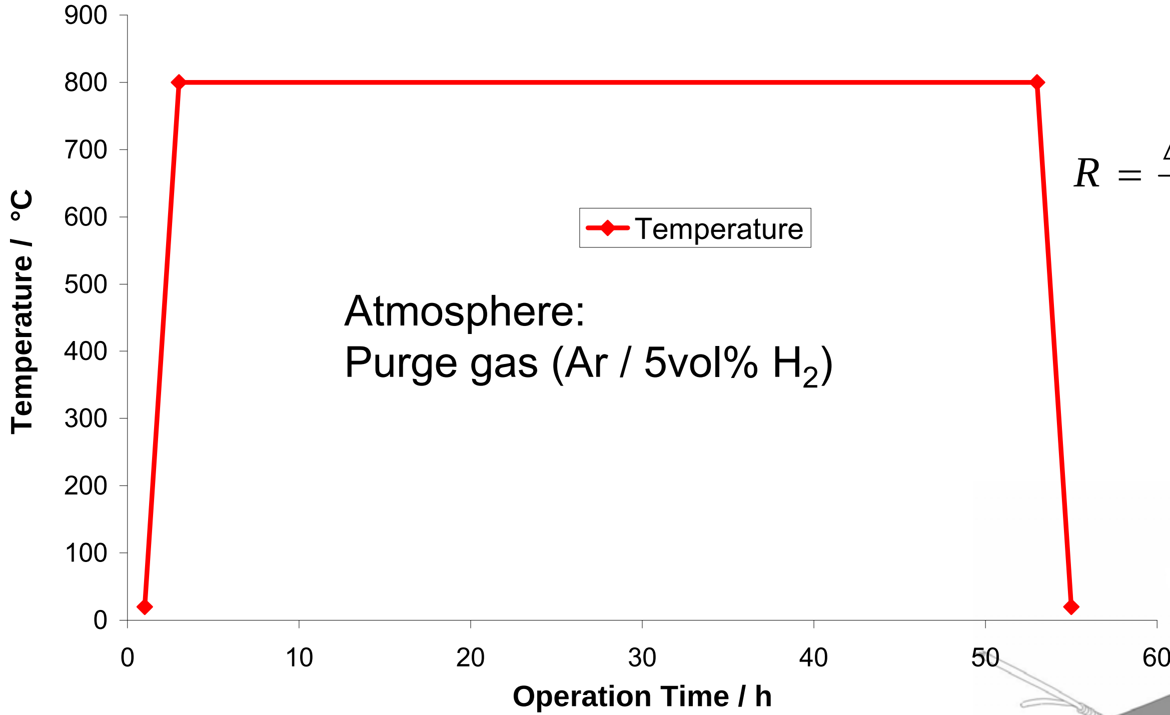

$$R = \frac{\Delta U}{\Delta I} \Rightarrow \sigma_{el} = \frac{l}{R \cdot A} = \frac{\text{S}}{\text{cm}}$$

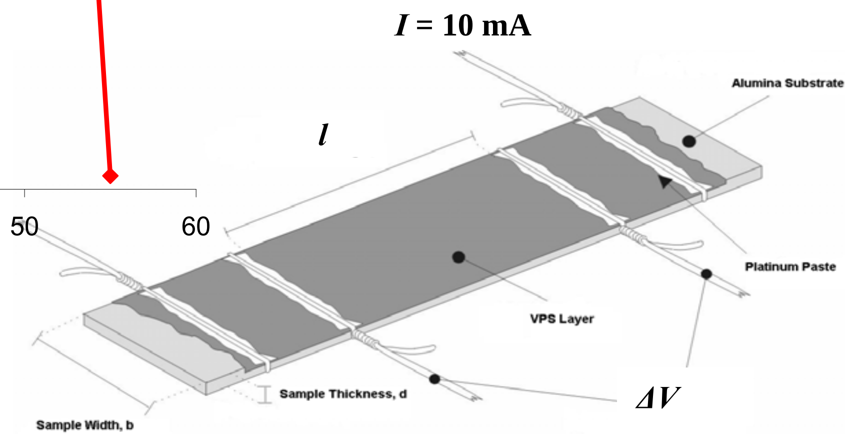

Electrochemical Testing of Full Cells

Operating temperature	800°C
Effective area	12.57 cm^2
Gas volume flow	
anode	0.5 slpm H_2 + 0.5 slpm N_2
cathode	2,0 slpm Air

1 SOFC
2 Gold sealing
3 Platinum net
4 Glass sealing
5 Housing
6 Weight